

Kidney International, Vol. 17 (1980), pp. 45-56

Morphologic alterations in the rat medullary collecting duct following potassium depletion

DAVID L. STETSON, JAMES B. WADE, and GERHARD GIEBISCH

Department of Physiology, Yale University School of Medicine, New Haven, Connecticut

Morphologic alterations in the rat medullary collecting duct following potassium depletion. Freeze-fracture and thin-section electron microscopy and morphometry were used to characterize further the response of the rat medullary collecting duct to potassium depletion. In freeze-fracture replicas, principal cells and intercalated cells were identified based on the assumption that intercalated cells possess a high density of rod-shaped intramembrane particles in their luminal membranes. Potassium depletion caused an increase in the relative number of cells with a high density of rod-shaped particles from the control level of 22% to 31% after 2 weeks and to 36% after 4 weeks. The frequency of intercalated cells identified by thin-section criteria was, however, about 35% in controls and unchanged by potassium depletion. This suggests that intercalated cells can have two types of membrane morphology. In potassium depletion, all intercalated cells display a high density of rod-shaped particles in their luminal membranes. In addition, the luminal membrane area of intercalated cells increased more than threefold, and the density of their rod-shaped particles increased by 21%. These observations suggest that the intercalated cell and its rod-shaped particle may be involved with the potassium reabsorption that occurs in this nephron segment with potassium depletion.

Modifications morphologiques du canal collecteur du rat consécutives à une déplétion en potassium. Le cryo-découpage, la microscopie électronique sur coupes fines et la morphométrie ont été utilisés pour mieux établir la réponse du canal collecteur médullaire du rat à la déplétion en potassium. Sur les répliques de cryo-découpage les cellules principales et les cellules intercalaires ont été identifiées à partir de l'hypothèse selon laquelle les cellules intercalaires possèdent une grande densité de particules intra-membranaires lumineales en forme de bâtonnets. La déplétion en potassium a déterminé une augmentation du nombre relatif de cellules de ce type de 22% chez les témoins à 33% après 2 semaines et 36% après 4 semaines. La fréquence des cellules intercalaires identifiées sur coupes minces, cependant, était de 35% chez les contrôles et non modifiés par la déplétion en potassium. Cela suggère que les cellules intercalaires peuvent avoir deux types de morphologies membranaires. Dans la déplétion en potassium toutes les cellules intercalaires ont une grande densité de particules en forme de bâtonnets dans leurs membranes lumineales. De plus, la surface membranaire lumineale des cellules intercalaires augmente de plus de trois fois et la densité des particules augmente de 21%. Ces observations suggèrent que les cellules intercalaires et leurs particules en forme de bâtonnets peuvent être impliquées dans la réabsorption de potassium qui prend place dans ce segment du néphron au cours de la déplétion en potassium.

Since the early reports that two cell types exist in the mammalian collecting duct [1], many investiga-

tors have attempted to define the morphologic characteristics and physiologic roles of these two cell types. The cell type known as principal cells or light cells are so named because they are the most numerous cell type in the collecting duct, and their cytoplasm stains lightly by both light microscopic and electron microscopic stains [2-4]. Electron microscopy has shown that principal cells have a paucity of cytoplasmic organelles and a relatively smooth luminal plasmalemma. In contrast, the intercalated cells, which are also called dark cells, take up stain more avidly, usually have many mitochondria, many apical cytoplasmic vesicles, and a luminal plasmalemma displaying dense microvilli or microplicae. Also, the cytoplasmic side of the luminal membrane and some apical vesicles of intercalated cells have regularly-spaced densities of unknown significance [4, 5] known as "studs" or "pegs." Principal cells and intercalated cells can be discriminated by scanning electron microscopy by virtue of the different morphologies of their luminal membranes [6, 7]. In addition, freeze-fracture studies [8] have suggested that only intercalated cells possess distinctive rod-shaped intramembrane particles, whereas principal cells possess unusual square particle arrays in their basolateral membranes.

Relying on some of these identification criteria, many investigators have studied the differential responses of these two cell types to various experimental or pathologic conditions. Oliver et al [9], using light microscopic criteria, demonstrated that potassium-depleted rats show an increase in the number of intercalated cells in the outer medullary

Received for publication February 2, 1979
and in revised form May 23, 1979

0085-2538/80/0017-0045 \$02.40

© 1980 by the International Society of Nephrology

collecting ducts. In fact, many experimental treatments are purported to cause increases in the relative frequency of intercalated cells. These experiments and their results are reviewed by Richet and Hagege [10].

Many previous attempts to quantify changes in intercalated cell number have relied on light microscopic identification of cell type. Unfortunately, the criteria by which principal cells and intercalated cells have been identified have some ambiguity and have led to controversy [5-7, 11, 12]. In particular, individual cells with characteristics of *both* principal and intercalated cells have been found in control and different experimental conditions [5-7]. These observations have been interpreted to mean that intercalated cells may represent a specific functional state of principal cells. Another possible interpretation of these observations, however, not yet considered, is that the two cell types in fact are distinct, but that appearance of intercalated cells may depend on functional demand at the cellular level.

This study extends the investigation of the response of the collecting duct to potassium depletion by using not only thin section but also freeze-fracture electron microscopy to identify principal cells and intercalated cells and to determine their relative incidence. In addition, the significance of the rod-shaped particles was investigated by assessing possible changes in the density of these particles and in the amount of luminal membrane possessing these distinctive particles. Ultrastructural morphometric data were also collected to characterize further the response of the collecting duct to potassium depletion.

Methods

Male Sprague-Dawley rats, each weighing 200 to 250 g, were fed Teklad potassium-deficient diet (no. 170550) for 2 or 4 weeks with tap or distilled water ad lib. Paired control animals were fed either Purina lab chow or Teklad potassium-control diet (no. 170555). Results in both control groups were indistinguishable, and, hence, pooled.

At the time of sacrifice, the animals were anesthetized with Inactin (Byk Gulden, Konstanz), 100 mg/kg body wt. Blood samples were taken from the carotid artery from some animals for determination of serum potassium. The kidneys were then fixed with vascular perfusion. (1) Karnovsky's fixative [13], diluted 1:3 with 0.1 M cacodylate buffer (pH, 7.2) was perfused through the entire body via a cannula inserted into the aorta through a cut in the wall of the left ventricle. Perfusion pressure was 50 mm

Hg. (2) The retrograde perfusion method of Bohman [14] was used with his fixative adjusted to 600 mOsm perfused at 200 mm Hg. Often, the first method did not flush the kidneys quickly or adequately, indicating a possibility of poor fixation. Such kidneys were discarded. The second method was used to improve the yield of well-fixed tissues. Also, we wanted to eliminate the chance that any observed change in morphology was due to poor fixation. The second method was compared to the first to identify inadequate fixation. Ultimately, no morphologic differences were observed between tissues fixed by the two perfusion methods.

Electron microscopy. Slices of tissue 1-mm thick were taken from the inner stripe of the red medulla. Tissue to be examined by freeze-fracture was soaked in 25% glycerol in 0.1 M cacodylate buffer for 2 to 18 hours. Samples were frozen in a frozen nitrogen slush produced by cooling liquid nitrogen to its freezing point under vacuum. Freeze-fracture replicas were prepared in a Balzers BAF 301 freeze-fracture apparatus using a Balzers mirror-image replica device. The thickness of the platinum-carbon and carbon films was controlled by a Balzers QSG 201 quartz-crystal thin-film monitor. Replicas were washed overnight in Chlorox, picked up on 100-mesh formvar-coated grids, and coded to eliminate bias during examination and quantification.

Tissue for conventional thin-section EM was prepared from the same kidneys and region as the freeze-fracture specimens. Tissue was postfixated with 1% osmium tetroxide, dehydrated in a graded series of ethanol, embedded in Durcupan ACM, and sectioned with a Diatome diamond knife (Electron Microscopy Sciences) and an LKB-Huxley ultramicrotome. Electron microscopy was performed with a Zeiss EM 10B microscope.

Quantification. Cell-type frequency from freeze-fracture replicas was estimated with either prints, negatives, or directly at the electron microscope. Because equivalent results were obtained with all these methods, most counts were obtained at the electron microscope at a magnification of $\times 10,000$. Cell counts from thin sections were determined only from prints. The identification of cell types in thin sections was tested by having independent appraisals carried out by two of us using the same prints. Essentially, identical estimates of cell frequencies were obtained. For both freeze-fracture replicas and thin sections, at least 49 cells were counted for each animal. After all counts were completed, the code was broken, and total experimental and control cell counts were tabulated.

Quantitation of intramembrane particle density was performed on at least 10 cells for each animal by using micrographs of appropriately fractured luminal membrane enlarged to $\times 54,000$. Membrane length was estimated on prints at $\times 5600$ from intersections of the membranes with a semicircular grid (after Merz, 15) with spacing of 1 cm. Because this test system has an isotropic line density for all orientations of the grid, use of this grid eliminates errors arising from the anisotropic orientation of membranes in epithelia. Boundary length (B), measured in micrometers, was determined by using the formula: $B = I_i \cdot d$, where I_i is the number of intersections with the test grid lines and the spacing (d) is equal to $1.786 \mu\text{m}$. Cell area, volume-percent (V_v) of organelles and inclusions, and surface density (S_v) were determined by stereologic analysis [16] by using a square array of points with spacing of 1 cm.

Statistics. Significance levels for cell counts were determined by using the χ^2 statistic, for particle density by using analysis of variance (ANOVA), and for other quantification by using Student's *t* test. All results are reported as the mean \pm SEM.

Results

Thin-section electron microscopy. The two main cell types described by previous investigators could be distinguished in thin sections of collecting ducts from the inner stripe of the outer medulla. Principal cells have a smooth luminal membrane and few cytoplasmic organelles (Fig. 1). Intercalated cells have a more amplified luminal membrane and more cytoplasmic organelles and inclusions (Fig. 1). As previously reported [4, 5], intercalated cells display distinctive studs associated with the cytoplasmic surfaces of the luminal plasmalemma and apical vesicles (Fig. 2). We found that the incidence of studs in membranes of intercalated cells is variable; this variability can be found in different animals fixed by different methods. The studs may occur only in vesicles and not in luminal membrane (Fig. 2a), in vesicles, and in discrete patches on the luminal plasmalemma (Fig. 2b), or associated with most of the plasmalemma. The plasmalemma of intercalated cells from potassium-depleted animals are always entirely studded and vesicles are largely absent from the apical cytoplasm (Fig. 2c). Studded vesicles appear dissimilar to pinocytotic-coated vesicles with respect to overall shape and size. Principal cells apparently do not have studded vesicles or plasmalemmal studs (Fig. 2d).

Freeze-fracture electron microscopy. Two cell types are also identifiable by freeze-fracture EM if

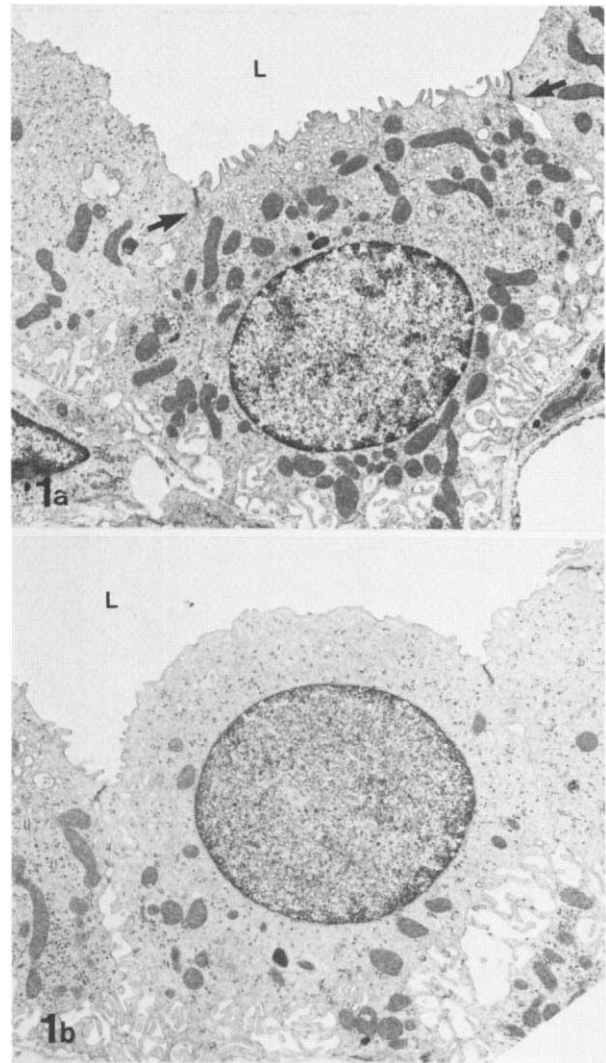


Fig. 1. Thin-section electron micrographs of the two main cell types in control rat medullary collecting duct. **a** Intercalated cell. Note the amplification of the luminal membrane and the large number of vesicles in the apical cytoplasm (between arrows). **b** Principal cell. This cell type has a rather smooth luminal membrane and unremarkable cytoplasm. (L, lumen; magnification $\times 5900$).

only luminal membrane characteristics are considered: (1) a cell type with a low density of intramembrane particles on the P fracture face of the luminal membrane (most of these particles are spherical but about 15% of them are rod-shaped) (Fig. 3), and (2) a cell type with a high density of rod-shaped particles on the luminal P face and corresponding depressions on the E face (about 35% of the total particles are spherical) (Fig. 4, a to c). Humbert et al [8] have suggested that intercalated cells have high-density rod-shaped particles and principal cells have none. It is clear from our work, however, that

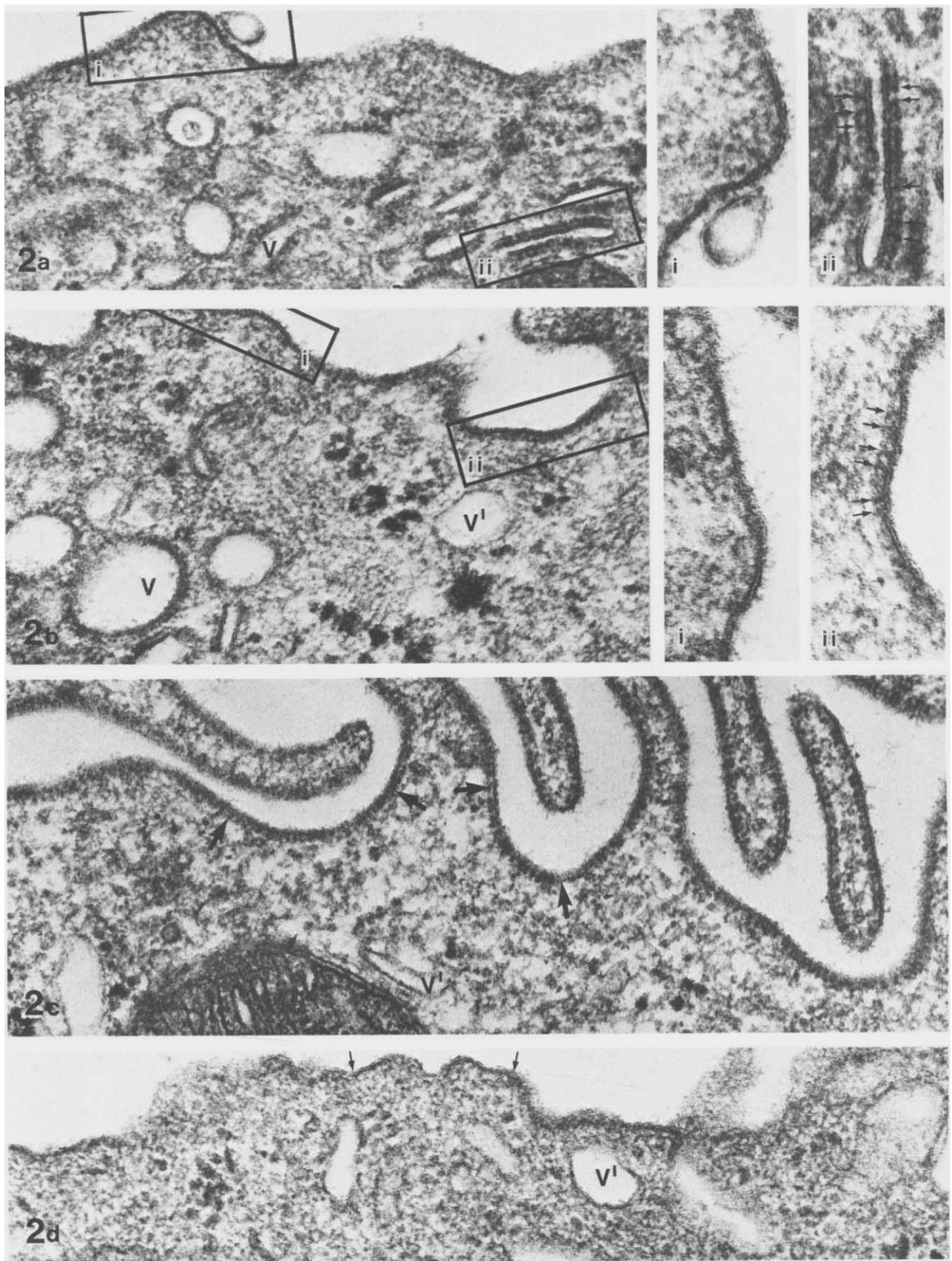


Fig. 2. Thin-section electron micrographs of the luminal regions of intercalated cells (a and b are control; c, potassium-depleted) and a principal cell (d). **a** Studs are not apparent on luminal membrane (inset i) but are clearly present on cytoplasmic vesicles (V and inset ii, arrows). The luminal membrane is without microvilli. **b** Studs are absent from most of the luminal membrane (inset i) and some apical vesicles (V'), but can be found on other vesicles (V) and in small patches on the luminal membrane (inset ii, studs, arrows). **c** Potassium-depleted intercalated cells have long microvilli, which are entirely coated with studs on their cytoplasmic side (arrows). Vesicles do not have studs (V'). **d** Principal cells possess no luminal membrane (arrows) or vesicle (V') studs. (Magnification: $\times 100,000$; insets, $\times 175,000$)

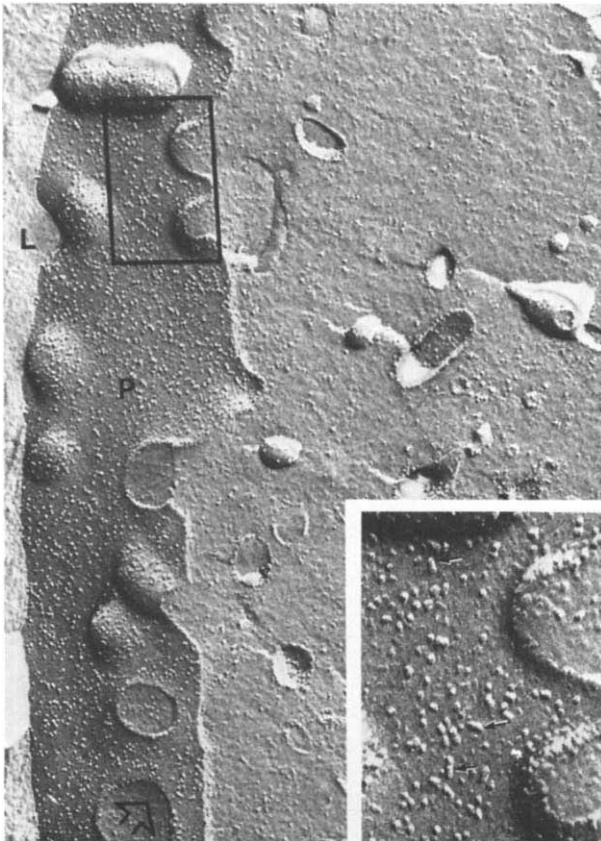


Fig. 3. Freeze-fracture replica of a control principal cell. The luminal membrane P fracture face (P) is characterized by a sparse population of particles, mostly spherical but with a few individual rod-shaped particles (*inset, arrows*). Apical vesicles have few rod-shaped particles. Large arrow indicates the direction of shadow. (L, lumen; magnification: $\times 54,000$; inset, $\times 125,000$)

structurally similar rod-shaped particles do occur in nearly all collecting duct cells, although infrequently in some cells. It is not clear, however, whether the rod-shaped particles of principal cells are functionally identical to those of intercalated cells.

The description of principal cells and intercalated cells in freeze-fracture becomes more complicated if one considers the cytoplasmic vesicles in addition to luminal membrane features. Some cells with a low density of rod-shaped particles in their apical plasmalemma have vesicles with high-density rod-shaped particles in their apical cytoplasm (Fig. 4d). Further, high-density rod-shaped particle cells can also have high-density rod-shaped particle vesicles in the apical cytoplasm.

The relative frequencies of high-density rod-shaped particle cells determined from freeze-fracture replicas are reported in Table 1 in comparison with those of intercalated cells determined by thin-

section electron microscopy. There is poor correspondence between these values for control animals. This discrepancy may be explained by the fact that cells with studded cytoplasmic vesicles and with smooth unstudded luminal membranes are called intercalated cells in thin section, but the same cells are called low-density rod-shaped particle cells in freeze-fracture. By pooling the observations from both thin sections and freeze-fracture replicas, we conclude that intercalated cells may exist in at least two forms: (type I) with high-density rod-shaped particles and studs associated with the luminal membrane, and (type II) without high-density rod-shaped particles or studs associated with the luminal membrane, but with them in cytoplasmic vesicles. Also, principal cells never have a high-density of rod-shaped particles or studs associated with either luminal membrane or cytoplasmic vesicles.

Response to potassium depletion. After 4 weeks of exposure to the potassium-deficient diet, rats are significantly depleted of potassium. Control animals have serum potassium concentrations of 3.6 ± 0.2 mmoles/liter, whereas 4-week potassium-depleted animals have serum potassium concentrations of 1.7 ± 0.2 mmoles/liter. As previously reported [17], potassium-depleted animals have not gained weight at the same rate as controls.

Response to potassium depletion seen by thin-section EM. Following potassium-depletion, intercalated cells show reduced incidence of studded vesicles in the apical cytoplasm, though pinocytotic vesicles and smooth endoplasmic reticulum remain (Fig. 2c). The apparent length of intercalated cell microplasm has increased as has the volume of most collecting duct cells (Fig. 5). These qualitative observations are confirmed by quantitative morphometry (Table 2). The luminal membrane boundary length of intercalated cells has increased by a factor of 3.3 after 4 weeks of potassium depletion. This effect appears to be highly specific because neither the principal cell luminal boundary length, principal cell basolateral boundary length, nor the intercalated cell basolateral boundary length shows a significant change during the same treatment. The mean area of both principal and intercalated cells in thin-section (an index of cell volume) approximately doubled following treatment. Cell enlargement was reported earlier by Oliver et al [9] and Muehrcke and Rosen [17]. Thus, all the cells of the medullary collecting duct from potassium-depleted animals are enlarged (Fig. 5), perhaps in response to altered intracellular ion composition. Although it is possible that this enlargement is due to poor tissue

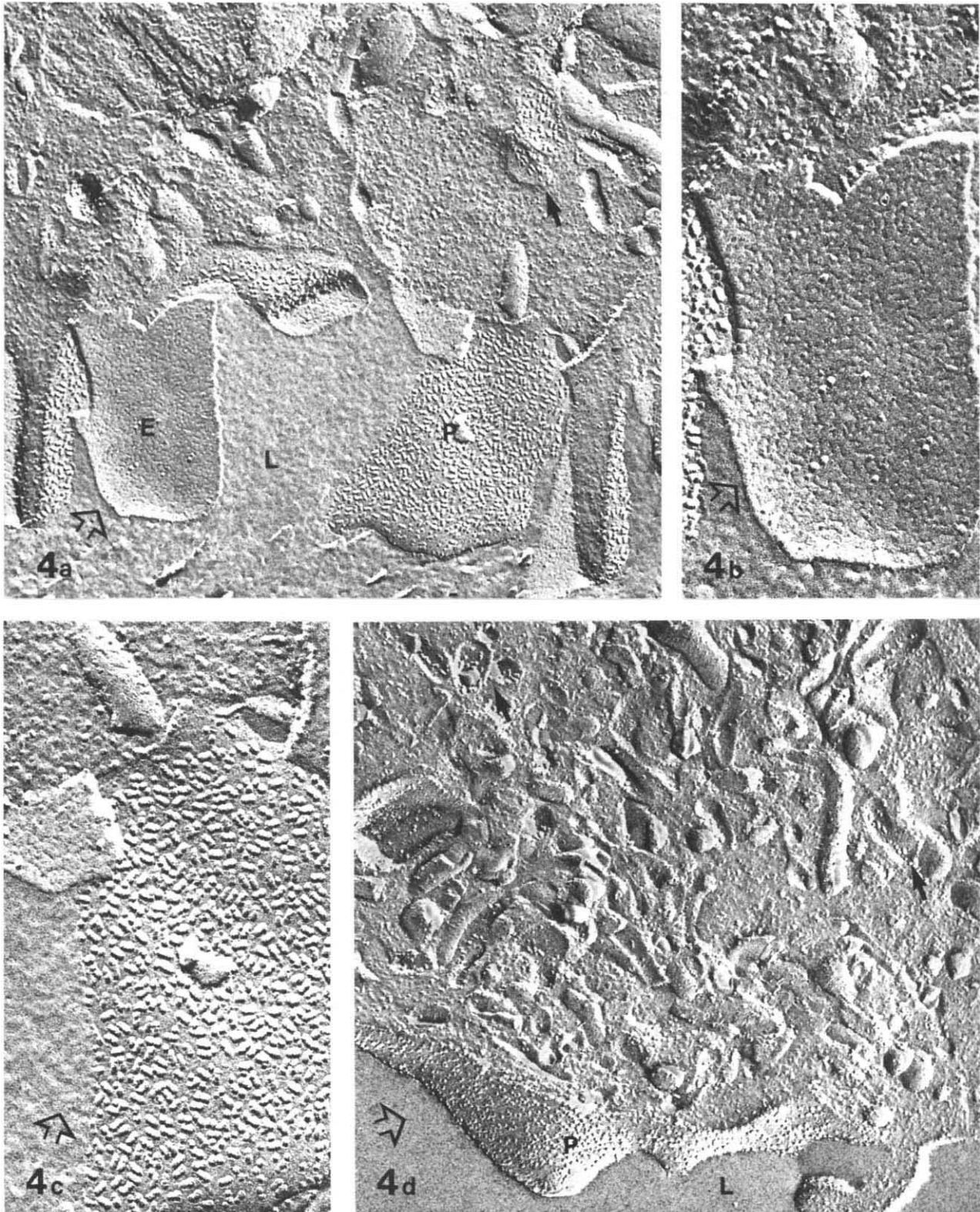


Fig. 4. Freeze-fracture replicas of control intercalated cells. **a** An intercalated cell with high-density rod-shaped particles in the luminal membrane. **b** and **c** Enlargements of the E face (**b**) and P face (**c**) of the cell shown in **a**. The luminal membrane E face depressions are produced by P face rod-shaped particles. **d** An intercalated cell with low-density rod-shaped particles in the luminal membrane. Cytoplasmic vesicles (arrows, **a** and **d**) also have particles. Large arrows indicate the direction of shadow. (L, lumen; magnification: **a** and **d**, $\times 75,000$; **b** and **c**, $\times 150,000$)

fixation, we consider this unlikely. Cells from potassium-depleted kidneys were enlarged consistently after both fixation methods, and none of the control kidneys showed enlargement that could be a fixation artifact. The possibility cannot be ruled out, however, that fixation of potassium-depleted kidneys differ from control kidneys because of altered renal hemodynamic factors.

The luminal surface density (S_v) of principal cells and the basolateral and total S_v of both principal cells and intercalated cells decreases. In contrast, the value of luminal S_v for intercalated cells tends to increase in spite of the large increase in cell volume, although this increase is not statistically significant.

Coincident with the increase in luminal membrane boundary length is an 80% decrease in the volume percent (V_v) of clear vesicles in the cytoplasm of intercalated cells (Table 3). A similar decrease does not occur in principal cells. The V_v of mitochondria in principal cells increases slightly following 4 weeks of potassium depletion. Also, intercalated cells have a larger V_v of mitochondria ($P < 0.01$, by t test) than do principal cells under control and potassium-depleted conditions, but it is not clear that the difference is large enough to serve as a reliable criterion for cell-type identification. Finally, the number of lysosomes in intercalated cells increases dramatically following potassium depletion, as previously reported by others [9, 18].

Response to potassium depletion seen by freeze-fracture EM. Freeze-fracture investigations of kid-

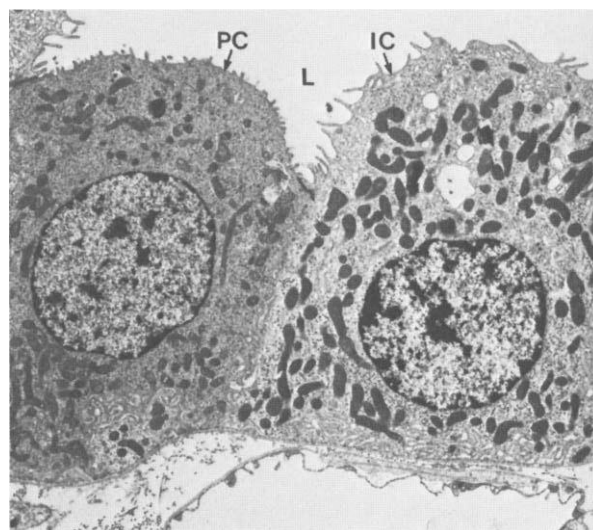


Fig. 5. A thin-section electron micrograph of a principal cell (PC) and an intercalated cell (IC) from a 4-week potassium-depleted rat. Both cell types are enlarged. The intercalated cell has longer luminal microvilli than control (cf. Fig. 1). (L, lumen; magnification, $\times 4000$)

neys from potassium-depleted animals show that the frequency of high-density rod-shaped particle cells increases from 22% in controls to 31% in animals depleted of potassium for 2 weeks and to 36% for 4-week depleted animals (Table 4). Note that the frequency of high-density rod-shaped particle cells seen in freeze-fracture is nearly identical to the frequency of intercalated cells seen in thin section in potassium-depleted animals (Table 1). Therefore, all intercalated cells have high-density rod-shaped particles as well as luminal microvilli and studs as noted in thin section; that is, one population of intercalated cells exists in potassium-depleted animals. In addition to an increase in the number of high-density rod-shaped particle cells, by 4 weeks of depletion the density of rod-shaped particles in these cells increases from the control level of 1792 ± 104 to 2173 ± 50 particles/ μm^2 with a commensurate increase in total particle density (Table 5, Fig. 6). Most of this increase occurs during the second 2 weeks of potassium depletion. A small increase in the incidence of luminal membrane spherical particles, and therefore total particles, occurs in low density rod-shaped particle cells by 2 weeks with no further increase occurring thereafter. In contrast, we observed no effect of potassium depletion on basolateral membrane morphology. Freeze-fracture replicas also show that the microvilli of high-density rod-shaped particle cells increase in length following potassium depletion (Fig. 7).

Table 1. Thin section vs. freeze-fracture evaluation of cell types (as percent of total)^a

Animals	Frequency of intercalated cells in thin section	Frequency of HRP cells in freeze-fracture
Control		
1	39% (149)	20% (70)
2	27 (103)	16 (128)
3	30 (79)	25 (72)
4	—	28 (102)
5	—	18 (67)
6	—	23 (105)
7	37 (125)	—
8	36 (72)	—
Total	34% (528)	22% (544) ^b
4-Week potassium depleted		
1	34% (113)	35% (136)
2	25 (134)	36 (124)
3	37 (324)	42 (59)
4	42 (95)	34 (312)
Total	35% (666)	36% (631)

^a Number in parentheses is number of cells counted. HRP is high-density rod-shaped particle.

^b $P < 0.001$ (χ^2), thin-section vs. freeze-fracture.

Table 2. Membrane morphometry^a

	Boundary length, μm		Cell area μm^2	$S_v, \mu\text{m}^{-1}$		
	Luminal	Basolateral		Luminal	Basolateral	Total
Principal cells						
Control (5)	13.2 \pm 1.4	90.9 \pm 8.4	47.1 \pm 7.7	0.40 \pm 0.07	2.68 \pm 0.29	3.08 \pm 0.34
4-Week K ⁺ depleted (6)	15.2 \pm 1.3	99.3 \pm 6.0	100.5 \pm 14.9	0.22 \pm 0.04	1.41 \pm 0.19	1.63 \pm 0.23
<i>P</i>	NS	NS	<.02	<0.05	<0.01	<0.01
Intercalated cells						
Control (5)	23.3 \pm 0.5	84.0 \pm 4.8	53.8 \pm 10.7	0.67 \pm 0.13	2.19 \pm 0.25	2.86 \pm 0.35
4-Week K ⁺ depleted (6)	76.9 \pm 13.4	88.2 \pm 15.6	112.9 \pm 25.0	0.95 \pm 0.11	1.15 \pm 0.21	2.11 \pm 0.25
<i>P</i>	<0.01	NS	<0.05 ^b	NS	<0.02	NS

^a Numbers in parentheses are the number of animals per group. Values are mean \pm SEM.

^b Mann-Whitney U test.

Table 3. Organelles/inclusions volume percent (V_v)^a

	Clear vesicles	Mitochondria	Lysosomes
Principal cells			
Control (5)	0.8 \pm 0.3	9.5 \pm 0.9	0.6 \pm 0.3
4-Week K ⁺ depleted (6)	0.6 \pm 0.2	13.8 \pm 0.9	1.2 \pm 0.2
<i>P</i>	NS	<0.01	NS
Intercalated cells			
Control (5)	8.1 \pm 0.7	19.4 \pm 1.0	0.4 \pm 0.2
4-Week K ⁺ depleted (6)	1.7 \pm 0.6	23.7 \pm 0.6	2.9 \pm 0.4
<i>P</i>	<0.001	NS	<0.001

^a Numbers in parentheses are the number of animals in each group. Values are mean \pm SEM.

Discussion

This work addresses two main problems in collecting duct morphology and physiology: (1) the identification of cell types, and (2) the morphologic response of the collecting duct associated with potassium depletion.

The present investigation and that of Humbert et al [8] have shown that membrane structural features vary between different cells of this epithelium; that is, the cell types can be classified on the basis of rod-shaped particle density within the luminal membrane. It has been shown here, however, that cells that may be called intercalated cells by thin-section criteria (that is, dense cytoplasm, many mitochondria, and numerous apical vesicles) may not have a high-density of luminal membrane rod-shaped particles. Therefore, we suggest that two populations of intercalated cells exist simultaneously in control rats; one population of cells with the characteristics of intercalated cells in thin section but without luminal membrane high-density rod-shaped particles, and a second population of intercalated cells that does have high-density rod-shaped particles in the luminal membrane. A similar division of intercalated cells into two types, "gray" and "dark," was previously suggested by Kriz, Kaisling, and Pszolla [19].

Potassium depletion, which has been shown to stimulate potassium reabsorption along nephron sites beyond the distal tubule [20-22], also causes a specific shift in the intercalated cell population such that all intercalated cells have a high density of luminal rod-shaped particles. This implies that the high-density rod-shaped particle-intercalated cell is a stimulated or differentiated form of intercalated cell. It is possible, but not proven, that potassium reabsorption may be a function of these cells in the collecting duct. The absence of change in the total intercalated cell population seen by thin-section in this study (Table 1) and also that of Hansen, Tisher, and Robinson [12] may indicate that the total number of intercalated cells is not altered by potassium depletion, but that the changes in incidence previously reported may reflect a modulation of cell structure within a constant intercalated cell population.

Prolonged potassium depletion also increases rod-shaped particle density and luminal plasma-membrane surface area only in intercalated cells.

Thus, there is an increase in total rod-shaped particle number in potassium depletion which can be attributed to compensatory increases at three levels: (1) an increase of particle density of 21%, (2) a three-fold increase in the luminal surface area of in-

Table 4. Incidence of cell types^a

Animal	HRP	LRP	Total	HRP % total
1	14	56	70	20
2	21	107	128	16
3	18	54	72	25
4	28	74	102	28
5	12	55	67	18
6	24	81	105	23
Total	117	427	544	22
2-Week potassium depleted				
1	34	62	96	35
2	44	78	122	36
3	21	56	77	27
4	22	42	64	34
5	63	173	236	27
6	14	35	49	29
7	18	38	56	32
Total	216	484	700	31 ^b
4-Week potassium depleted				
1	47	89	136	35
2	44	80	124	36
3	24	34	59	42
4	105	207	312	34
Total	220	410	630	36 ^b

^a Abbreviations are: HRP, high-density rod-shaped particle cells; and LRP, low-density rod-shaped particle cells.

^b $P < 0.005$ (χ^2).

tercalated cells, and (3) a 60% increase in the number of intercalated cells with a high density of rod-shaped particles. These summed increases yield a sixfold increase in the total rod-shaped particle number in the outer medulla. At the same time, principal cells display a 30% increase in spherical particle number, no change in luminal surface area, and no change in total number of cells within the collecting duct. Therefore, there is only a 1.3-fold increase in spherical particle number. The increase in rod-shaped particles seems to be a specific re-

Table 5. Luminal membrane particle densities (no. particles/ μm^2)^a

	Spherical	Rod-shaped	Total
LRP cells			
Control (5,29)	1101 \pm 59	199 \pm 26	1301 \pm 64
2-Week (7,64)	1467 \pm 47	176 \pm 18	1643 \pm 55
4-Week (4,47)	1431 \pm 86	216 \pm 25	1647 \pm 103
P	<0.01	NS	<0.05
HRP cells			
Control (5,22)	963 \pm 90	1792 \pm 104	2756 \pm 90
2-Week (7,60)	999 \pm 51	1852 \pm 50	2847 \pm 53
4-Week (4,56)	860 \pm 46	2173 \pm 50	3033 \pm 42
P	NS	<0.01	<0.01

^a Numbers in parentheses are the number of animals in each group, with the total number of cells for that group. Abbreviations are: LRP, low-density rod-shaped particle; and HRP, high-density rod-shaped particle.

sponse by the kidney to potassium depletion. Table 6 summarizes the characteristics of the cell types and the changes that occur after potassium depletion.

An explanation for the increase in intercalated cell luminal membrane may be deduced from the behavior of their studded cytoplasmic vesicles. Freeze-fracture indicates that these vesicles possess rod-shaped particles. The vesicles are not present in potassium-depleted intercalated cells, though the luminal plasmalemma, which was variably studded in control cells, is now entirely studded. This raises the possibility that studded vesicles can fuse with the luminal plasmalemma, contributing both membrane and rod-shaped particles. The stimulus for the proposed fusion of studded vesicles with intercalated cell luminal membrane is unknown, but it may be a fall in intracellular potassium concentration caused by organismal potassium depletion.

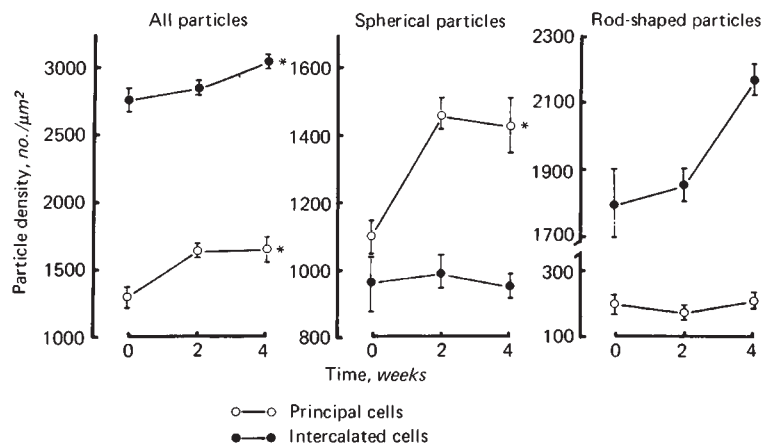


Fig. 6. A graphical demonstration of the increases in luminal membrane particle density with duration of K^+ depletion. Asterisk denotes P at least < 0.05 by analysis of variance.

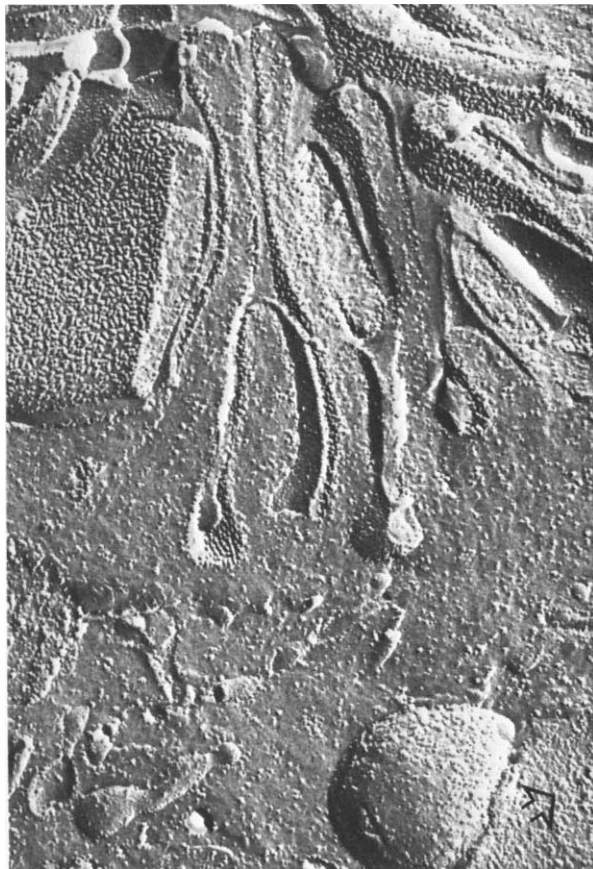


Fig. 7. A freeze-fracture replica of a 4-week K^+ depleted intercalated cell. The microvillae are longer, the rod-shaped particles denser, and the apical cytoplasmic vesicles with rod-shaped particles fewer than the control (cf. Fig. 4). (Magnification, $\times 52,000$)

Rod-shaped intramembrane particles have also been described in flask cell in *Xenopus* kidney [23] (and unpublished observations) and in the mitochondria-rich cell of toad bladder [24, 25]. The fact that studs have also been found in association with

the membranes of these cell types in thin sections [26, 27] is consistent with the association of these two features found in the present work. It has been suggested that *Xenopus* flask cells are involved in ion regulation [28] and/or acid-base and nitrogen balance [29]; toad bladder mitochondria-rich cells are also believed to be involved with urinary acidification [30, 31]. The evidence of the present work combined with these other studies argues that the rod-shaped particle and associated stud may mediate potassium ion and/or hydrogen ion transport.

Potassium depletion in rats has been shown to be associated with marked chronic metabolic alkalosis [32], with enhanced proximal tubular bicarbonate reabsorption and hydrogen ion secretion [33, 34]. Although there is no direct evidence of increased acidification by the collecting duct, potassium depletion has recently been found to stimulate excretion of ammonia by the distal nephron [35]. Therefore, it is possible that the morphologic response reported here is related to a change in bicarbonate, hydrogen, and/or ammonium ionic transport rather than with potassium reabsorption. But, because of a close relationship between acid-base balance and potassium transport, it is also possible that the handling of the four ions, potassium, bicarbonate, ammonium, and hydrogen, is mediated by an inter-related transport system within intercalated cells.

Wade et al [36] have just shown that long-term treatment of rabbits with desoxycorticosterone acetate (DOCA) causes a dramatic amplification of the basolateral membrane of principal cells in cortical collecting tubules. DOCA also causes an increase in sodium reabsorption and potassium secretion by the same tubules [37]. Moreover, Silva, Hayslett, and Epstein [38] have shown that potassium loading in rats induces increases in medullary sodium-po-

Table 6. Summary of cell-type characteristics

Cell type	Approx. relative frequency of cell type, %	Cell luminal surface area ^a	Luminal membrane ^a		Apical vesicles ^a	
			High-density rod-shaped particles	Studs	High-density rod-shaped particles	Studs
Control						
Principal	65	—	0	0	0	0
Intercalated type I	20	—	+	+	+	+
Intercalated type II	15	—	0	0	+	+
K^+ depleted						
Principal	65	NC	0	0	0	0
Intercalated type I	35	++	++	+	±	±
Intercalated type II	0	—	—	—	—	—

^a0, denotes not present; +, present; NC, no change; ++, increase; and ±, variably present.

tassium-ATPase. Potassium loading also causes an increase in basolateral surface area in medullary collecting ducts in rats [39]. In contrast, potassium depletion causes an increase in the luminal surface area of intercalated cells with no concomitant change in principal cells. This collected evidence suggests that principal cells are involved with reabsorption of sodium and secretion of potassium, that intercalated cells are responsible for the reabsorption of potassium and perhaps also the secretion of hydrogen ions, and that the balance of the two separate functions contributes to the determination of the final urine potassium concentration and pH.

Summary (Table 6). This study has demonstrated: (1) that two populations of intercalated cells exist in the rat medullary collecting duct, (2) that potassium depletion induces an increase in the incidence of intercalated cells having a high density of rod-shaped particles in their luminal membrane, (3) that the area of luminal plasmalemma of intercalated cells increases in potassium depletion, and (4) that the density of rod-shaped particles in intercalated cell luminal membrane increases in response to potassium depletion.

Acknowledgments

This work was supported by U.S. Public Health Service Grants #AM 19344 and #AM 17433, and by a Research Career Development Award (5-KO4-AM 00217) granted to Dr. J. B. Wade. Ms. J. Pryor gave technical assistance, and Ms. L. Kiesewetter and B. Frank prepared the manuscript. Dr. M. Farquhar helped review this manuscript.

Reprint requests to Dr. D. L. Stetson, Department of Physiology, Yale University School of Medicine, New Haven, Connecticut 06510, USA

References

1. SjöSTRAND F: Über die Eigenfluoreszenz tierischer Gewebe mit besonderer Berücksichtigung der Saugertierniere. *Acta Anat (Basel)* 1 (suppl. 1):1-163, 1944
2. MöLLENDORF WV: Der Excretionapparat, in *Handbuch der Mikroskopischen Anatomie des Menschen*, edited by MöLLENDORF WV, Berlin, Julius Springer, vol. 7, part 1, 1930
3. RHODIN JAG: Anatomy of kidney tubules. *Int Rev Cytol* 7:485-534, 1958
4. GRIFFITH LD, BULGER RE, TRUMP BF: Fine structure and staining of mucosubstances on "intercalated cells" from the rat distal convoluted tubule and collecting duct. *Anat Rec* 160:643-662, 1968
5. MYERS CE, BULGER RE, TISHER CC, TRUMP BF: Human renal ultrastructure: IV. Collecting duct of healthy individuals. *Lab Invest* 15:1921-1950, 1966
6. HAGEGE J, GABE M, RICHT G: Scanning of the apical pole of distal tubular cells under differing acid-base conditions. *Kidney Int* 5:137-146, 1974
7. ORDONEZ NG, SPARGO BH: The morphologic relationship of light and dark cells of the collecting tubule in potassium-depleted rats. *Am J Pathol* 84:317-326, 1976
8. HUMBERT F, PRICAM C, PERRELET A, ORCI L: Specific plasma membrane differentiations in the cells of the kidney collecting tubule. *J Ultrastr Res* 52:13-20, 1975
9. OLIVER J, MACDOWELL M, WELT LG, HOLLIDAY MA, HOLLANDER W JR, WINTERS RW, WILLIAMS TF, SEGAR WE: The renal lesions of electrolyte imbalance: I. The structural alterations in potassium-depleted rats. *J Exp Med* 106:563-574, 1957
10. RICHT G, HAGEGE J: Dark cells of the distal convoluted tubules and collecting ducts: II. Physiological significance. *Fortschr Zool* 23:299-306, 1975
11. HUSER J, EVAN A, BENGELE HH, ALEXANDER EA: Effect of changes in potassium (K) metabolism on collecting system morphology. *Abst 11th Meeting Am Soc Nephrol*, 1978, p. 130A
12. HANSEN GP, TISHER CC, ROBINSON RR: Response of collecting ducts (CD) to disturbances of hydrogen ion and potassium balance. *Clin Res* 26:464A, 1978
13. KARNOVSKY MJ: A formaldehyde-glutaraldehyde fixative of high osmolality for use in electron microscopy. *J Cell Biol* 27:137A-138A, 1965
14. BOHMAN SO: The ultrastructure of the rat renal medulla as observed after improved fixation methods. *J Ultrastr Res* 47:329-360, 1974
15. MERZ WA: Die Streckenmessung an gerichteten Strukturen im Mikroskop und ihre Anwendung zur Bestimmung von Oberflächen-Volumen-Relationen in Knochengewebe. *Mikroskopie* 22:132-142, 1967
16. WEIBEL ER, BOLENDER RP: Stereological techniques for electron microscopic morphometry, in *Principles and Techniques of Electron Microscopy*, edited by HAYAT MA, New York, Van Nostrand Reinhold Co., 1973, vol. 3, pp. 237-296
17. MUEHRCKE RC, ROSEN S: Hypokalemic nephropathy in rat and man. *Lab Invest* 13:1359-1373, 1964
18. TOBACK FG, ORDONEZ NG, BORTZ SL, SPARGO BH: Zonal changes in renal structure and phospholipid metabolism in potassium-deficient rats. *Lab Invest* 34:115-124, 1976
19. KRIZ W, KAISLING B, PSZOLLA M: Morphological characterization of the cells in Henle's loop and the distal tubule, in *New Aspects of Renal Function*, edited by VOGEL HG, ULLRICH KJ, Amsterdam, Excerpta Medica, 1978, vol. 6, pp. 67-79
20. MALNIC G, KLOSE RM, GIEBISCH G: Micropuncture study of renal potassium excretion in the rat. *Am J Physiol* 206:674-686, 1964
21. DUARTE CG, CHOMETY F, GIEBISCH G: Effect of amiloride ouabain and furosemide on distal tubular function in the rat. *Am J Physiol* 221:632-639, 1971
22. FOWLER N, GIEBISCH G, WHITTEMBURY G: Distal tubular tracer microinjection study of renal tubular potassium transport. *Am J Physiol* 229:1227-1233, 1975
23. BROWN D: Freeze-fracture of *Xenopus laevis* kidney: Rod-shaped particles in the canalicular membrane of the collecting tubule flask cell. *J Ultrastr Res* 63:35-40, 1978
24. ORCI L, HUMBERT F, AMHERDT M, GROSSO A, DESOUSA RC, PERRELET A: Patterns of membrane organization in toad bladder epithelium: A freeze-fracture study. *Experientia* 31:1335-1338, 1975
25. WADE JB: Membrane structural specialization of the toad urinary bladder revealed by the freeze-fracture technique: II. The mitochondria-rich cell. *J Membr Biol* 26:111-126, 1976
26. STETSON DL: Physiological and morphological parameters

- of ammonia excretion in the kidney of *Xenopus laevis*. Ph.D. Thesis. Brown Univ., 1977
27. CHOI JK: Electron microscopy of absorption of tracer materials by toad urinary bladder epithelium. *J Cell Biol* 25:175-192, 1965
 28. SPANNHOF L: Wirkung osmotischer Belastung auf den Kralenfrosch *Xenopus laevis*. *Naturwissenschaften* 53:588-589, 1966
 29. STETSON DL: Renal alterations induced by osmotic stress and metabolic acidosis in *Xenopus laevis*. *J Exp Zool* 206:157-166, 1978
 30. ROSEN S, OLIVER JA, STEINMETZ PR: Urinary acidification and carbonic anhydrase distribution in bladders of Dominican and Colombian toads. *J Membr Biol* 15:193-205, 1974
 31. FRAZIER LW: Cellular changes in toad urinary bladder in response to metabolic acidosis. *J Membr Biol* 40:165-177, 1978
 32. COOKE RE, SEGAR WE, CHEEK DB, COVILLE FE, DARROW DC: The external correction of alkalosis associated with K deficiency. *J Clin Invest* 31:798-805, 1952
 33. KUNAU RT JR, FRICK A, RECTOR FC JR, SELDIN DW: Micropuncture study of the proximal tubular factors responsible for the maintenance of alkalosis during potassium deficiency in the rat. *Clin Sci* 34:223-231, 1968
 34. RECTOR FC JR: Renal acidification and ammonia production: chemistry of weak acid and bases; buffer mechanisms, chapter 9, in *The Kidney*, edited by BRENNER BM, RECTOR FC JR. Philadelphia, W. B. Saunders Co., 1976, vol. 1, p. 318
 35. KARLMARK B, JAEGER P, GIEBISCH F: Micropuncture study of tubular acidification and $\text{NH}_3\text{-NH}_4$ transport during chronic potassium (K) depletion. *Kidney Int* 14:766, 1978
 36. WADE JB, O'NEIL RG, PRYOR JL, BOULPAEP EL: Modulation of cell membrane area in renal collecting tubules by corticosteroid hormones. *J Cell Biol* 81:439-445, 1979
 37. O'NEIL RG, HELMAN SI: Transport characteristics of renal collecting tubules: Influences of DOCA and diet. *Am J Physiol* 233:F544-F558, 1977
 38. SILVA P, HAYSLETT JP, EPSTEIN FH: The role of $\text{Na}^+\text{-K}^+$ activated adenosine triphosphatase in potassium adaptation. Stimulation of enzyme activity by potassium loading. *J Clin Invest* 52:2265-2271, 1973
 39. KASHGARIAN M: Changes in cell membrane surfaces associated with alteration of transepithelial ion movement, in *Current Topics in Membranes and Transport*, New York, Academic Press, in press